Discover Oncology

Analysis

XGBoost model for predicting erectile dysfunction risk after radical prostatectomy: development and validation using machine learning

Hesong Jiang[1] · Lu Ji[1] · Leilei Zhu[2] · Hengbing Wang[1] · Fei Mao[1,3]

Received: 25 March 2025 / Accepted: 12 May 2025
Published online: 19 May 2025

Abstract

Background Erectile dysfunction (ED) is a frequent complication following radical prostatectomy, significantly affecting patients' quality of life. Traditional predictive methods often struggle to capture complex nonlinear risk factors. This study aims to develop a machine learning-based model to improve ED risk stratification and guide personalized management.

Methods A total of 1,147 prostate cancer patients were analyzed, among whom 285 (24.85%) developed postoperative ED. Univariate and multivariate analyses identified age, smoking history, Gleason score, prostate volume, T-stage, surgical approach, operative time, intraoperative bleeding, and PCT levels as independent risk factors ($P < 0.05$). Machine learning models, including XGBoost, Random Forest, Support Vector Machine, and k-Nearest Neighbors, were trained for ED risk prediction. Key predictors included advanced age, smoking history, Gleason score ≥ 8, prostate volume ≥ 40 ml, T-stage, laparoscopic-assisted surgery, and prolonged operative duration.

Results XGBoost exhibited the highest predictive accuracy (AUC: 0.980 in training; 0.960 in validation), outperforming other models. Calibration curves confirmed strong concordance between predicted and actual probabilities, while decision curve analysis demonstrated superior clinical utility, with XGBoost providing the greatest net benefit. Ten-fold cross-validation indicated stable performance (validation AUC: 0.9127 ± 0.0770; test AUC: 0.9592; accuracy: 0.9111), and external validation confirmed model generalizability (AUC: 0.84). SHAP analysis highlighted key risk contributors, enabling individualized risk assessment and targeted clinical interventions.

Conclusion The XGBoost model exhibited superior predictive performance and clinical applicability in assessing ED risk after radical prostatectomy, offering a robust tool for personalized postoperative management.

Keywords Erectile dysfunction (ED) · Radical prostatectomy · Machine learning · XGBoost model · Risk prediction

Supplementary Information The online version contains supplementary material available at https://doi.org/10.1007/s12672-025-02685-y.

✉ Hengbing Wang, wanghengbing2004@163.com; ✉ Fei Mao, maofeidoctor@njmu.edu.cn | [1]Department of Urology, The Affiliated Huaian No. 1 People's Hospital of Nanjing Medical University, Huaian City 223300, Jiangsu Province, China. [2]Department of Urology, The Affiliated Wuxi People's Hospital of Nanjing Medical University, Wuxi People's Hospital, Wuxi Medical Center, Nanjing Medical University, #299 Qingyang Road, Wuxi 214023, Jiangsu Province, China. [3]Department of Urology, The Affiliated Huaian No. 1 People's Hospital of Xuzhou Medical University, Huaian City 223300, Jiangsu Province, People's Republic of China.

1 Introduction

Prostate cancer stands among the most prevalent malignancies affecting men worldwide, with its incidence steadily rising due to advancing age, genetic predisposition, androgenic dysregulation, and lifestyle factors [1, 2]. According to GLOBOCAN data, it is the second most frequently diagnosed malignancy in men, surpassed only by lung cancer [3, 4]. Based on disease progression, prostate cancer is stratified into localized, locally advanced, and metastatic stages.

In clinical practice, radical prostatectomy (RP) remains the cornerstone of curative treatment for localized prostate cancer, offering significant reductions in mortality and prolonging survival [5, 6]. However, despite its oncological efficacy, RP carries the risk of iatrogenic injury to the adjacent neurovascular bundles, frequently resulting in debilitating postoperative complications such as erectile dysfunction (ED) [7, 8]. Beyond its physiological ramifications, ED imposes profound psychological and social burdens, engendering feelings of shame, anxiety, and helplessness that erode self-esteem and, in severe cases, precipitate depression. More critically, the protracted recovery following RP is further compounded by ED, exacerbating psychological distress and impeding the restoration of preoperative normalcy. Studies indicate that the prevalence of anxiety and depression is significantly higher among patients with postoperative ED than in those retaining sexual function [9, 10]. Moreover, ED may engender withdrawal from intimate relationships and social interactions, further amplifying psychological distress and diminishing overall quality of life.

The onset of ED following radical prostatectomy is predominantly attributed to neurovascular bundle (NVB) injury and disruption of the smooth muscle integrity within the corpora cavernosa [11, 12]. Anatomically, the dorsal and lateral surfaces of the prostate lie in close proximity to the pelvic autonomic plexus, rendering the delicate neural structures vulnerable to intraoperative trauma. Despite advancements in nerve-sparing (NS) techniques, surgical manipulation may still induce direct neural injury or traction-related damage, thereby compromising parasympathetic signaling critical for erectile function. Additionally, surgical disruption of the prostatic and penile arterial supply may diminish penile perfusion, precipitating cavernosal ischemia and subsequent erectile impairment. Postoperative local inflammatory responses further contribute to corporal fibrosis, exacerbating the functional decline. Notably, a subset of patients experiences a postoperative decline in testosterone levels, an endocrine perturbation that further undermines erectile capacity [13].

Traditionally, clinicians have relied on empirical judgment or conventional statistical models to predict and manage ED; however, these methodologies are inherently constrained by predefined assumptions and linear regression frameworks, limiting their capacity to capture the intricate, nonlinear interplay of contributory factors [14–16]. Machine learning algorithms hold remarkable promise for clinical prediction, particularly in navigating the complexities of multidimensional health data, where they excel at uncovering nonlinear relationships and latent patterns often elusive to traditional statistical approaches. Erectile dysfunction arises from an intricate interplay of physiological, psychological, and lifestyle factors, with variable relationships so complex that they frequently elude comprehensive capture by conventional modeling techniques. In contrast, machine learning methodologies integrate diverse data sources—including electronic health records, laboratory assessments, and medical histories—to enable individualized risk prediction for the onset of erectile dysfunction, thereby facilitating early intervention [17–20]. Nonetheless, the clinical implementation of machine learning remains fraught with challenges. Chief among these are the "black box" nature of certain models, which hampers interpretability and engenders skepticism among clinicians, and the limited generalizability of models, whose performance often fluctuates across centers and diverse populations. Moreover, clinical datasets are typically marred by noise, missing values, and class imbalance, all of which threaten model robustness and predictive fidelity. To address these limitations and enhance clinical applicability, the present study employed SHAP analysis to bolster model interpretability and leveraged multi-center data for external validation to rigorously evaluate generalizability. Through these optimization strategies, we aim to accelerate the clinical translation of machine learning technologies in the risk prediction of disorders such as erectile dysfunction.

Postoperative ED is modulated by an array of variables, including patient age, surgical technique, and anatomical variability, which conventional models struggle to simultaneously integrate and weigh. Leveraging its superior data-processing capabilities, machine learning not only facilitates the analysis of high-dimensional datasets but also autonomously identifies the most prognostically relevant features. More critically, the algorithms employed in this study extend beyond merely delineating risk factors; they enable precise, individualized risk stratification. Through the implementation of a SHAP-based personalized risk scoring system, clinicians can quantitatively assess each patient's likelihood of developing postoperative ED, allowing for the formulation of tailored intervention strategies. This data-driven approach enhances postoperative management and ultimately optimizes patient quality of life.

2 Materials and methods

2.1 Study subjects

The dataset for this study was sourced from the clinical databases of The Affiliated Huaian No. 1 People's Hospital and Wuxi People's Hospital, both affiliated with Nanjing Medical University.

Inclusion criteria: (1) Patients who underwent radical prostatectomy (either laparoscopic or robot-assisted) utilizing nerve-sparing techniques; (2) surgeries performed by senior surgeons with established proficiency in radical prostatectomy; (3) pathologically or radiologically confirmed localized prostate cancer, defined as tumors confined within the prostate without extracapsular extension, seminal vesicle invasion, or distant metastasis; (4) preoperative International Index of Erectile Function-5 (IIEF-5) score ≥ 22, or no documented history of erectile dysfunction.

Exclusion criteria: (1) Patients with concurrent malignancies; (2) patients with severe preexisting conditions impacting erectile function, including long-standing diabetes mellitus (> 10 years) with neurovascular complications, hypothyroidism, or central and peripheral neuropathies (e.g., Parkinson's disease, spinal cord injury); (3) patients who received postoperative androgen deprivation therapy (ADT) or pelvic radiotherapy; (4) patients who succumbed within 30 days postoperatively or developed severe complications (e.g., vesicocutaneous fistula, refractory urinary incontinence) precluding erectile function assessment; (5) patients with incomplete clinical records or loss to follow-up.

All patients were followed for a minimum of six months postoperatively. The Ethics Committee of Wuxi People's Hospital and The Affiliated Huaian No. 1 People's Hospital of Nanjing Medical University has approved this study (No: KY-2024-198-01). Given the retrospective study design, the institutional review boards waived the requirement for informed consent.

2.2 Study design and data collection

A total of 27 variables were collected across preoperative (within 24 h before surgery), intraoperative, and postoperative time points. Preoperative variables encompassed demographic characteristics (age, smoking history, alcohol consumption, and BMI), baseline clinical parameters (ASA score, NRS2002 score, surgical history, and family history), medical comorbidities (anemia, coronary artery disease, diabetes, hypertension, and hyperlipidemia), tumor-related features (pathological Gleason score, T stage, tumor size, and tumor distribution), and laboratory indices (albumin and PSA). Intraoperative variables included surgical approach, operative duration, and intraoperative blood loss. Postoperative variables comprised laboratory markers such as PSA, procalcitonin (PCT), C-reactive protein (CRP), neutrophil-to-lymphocyte ratio (NLR), and serum amyloid A (SAA). Notably, PCT, CRP, NLR, and SAA were measured within 48 h postoperatively, while PSA levels were assessed six months following surgery. The primary outcome of this study was erectile dysfunction.

2.3 Diagnosis of ED and definition of associated factors

This study utilized the IIEF-5 to diagnose and quantify the severity of ED [21–23]. The IIEF-5, a validated self-reported questionnaire, assesses multiple facets of erectile function, including erectile capacity and sexual satisfaction, based on the patient's experiences over the preceding six months. Comprising five items, each rated on a scale from 1 to 5, the questionnaire provides a robust evaluation of erectile function. At six months postoperatively, erectile function data were collected through WeChat, telephone interviews, or outpatient follow-up. Patients were stratified according to their IIEF-5 scores: those scoring < 22 were classified into the ED group, whereas those with scores ≥ 22 were assigned to the non-ED group.

2.4 Development and evaluation of predictive models for machine learning algorithms

SPSS and R software were employed to develop and evaluate the clinical prediction model. (1) Data Preprocessing. This study included prostate cancer patients treated at Wuxi People's Hospital between January 2020 and January 2025 as the internal validation cohort. Simultaneously, prostate cancer patients from The Affiliated Huaian No. 1 People's Hospital during the same period were selected as the external validation cohort. To ensure model robustness and generalizability, the internal validation cohort was randomly stratified into a training set (70%) and a test

set (30%). (2) Univariate and Multivariate Analysis. In the internal validation cohort, categorical variables were compared between groups using the chi-square test. Continuous variables following a normal distribution were analyzed using the t-test, whereas non-normally distributed continuous variables were assessed via the rank-sum test. A significance level of $P < 0.05$ was considered statistically significant. Additionally, four machine learning algorithms—Extreme Gradient Boosting (XGBoost), Random Forest (RF), Support Vector Machine (SVM), and k-nearest neighbor algorithm (KNN)—were employed to rank the importance of independent predictive factors. Each model assessed variable importance based on its internal algorithm, quantifying the contribution of each factor to the prediction of postoperative ED. In this study, variable importance scores were computed and ranked across multiple machine learning models. The selection of specific thresholds was guided by three principal considerations. First, to ensure model consistency and comparability, a unified threshold was established by selecting the top-ranked variable from each model, thereby avoiding selection bias arising from disparate model-specific criteria. Second, in pursuit of optimal model performance, preliminary analyses revealed that prioritizing top-ranked variables preserved critical information while mitigating the risks of overfitting and unnecessary model complexity. Iterative evaluations indicated that this threshold achieved the most favorable balance between predictive performance and interpretability. Third, to substantiate the appropriateness of the chosen threshold, models were retrained and evaluated under varying thresholds (e.g., top 5, top 15, and top 20 variables), with comparative analyses of key performance metrics (such as AUC and accuracy). Results consistently demonstrated that models utilizing the top-ranked variables achieved superior performance across both internal and external validation cohorts while preserving clinical utility. To facilitate comparison of feature importance across models, a normalization strategy was employed. Recognizing that different algorithms derive feature importance through disparate mechanisms (e.g., weight magnitudes in linear models versus feature scores in nonlinear models), we normalized each model's importance scores to a 0–1 range. The mean normalized score for each variable was then calculated across all models and ranked in descending order, ensuring a coherent and unified framework for cross-model comparison of feature importance. XGBoost and RF: Both ensemble learning methods leverage decision trees and assess variable importance through feature split contribution. These models determine a variable's significance by analyzing its frequency as a splitting node across all decision trees and its contribution to information gain (e.g., Gini index or entropy), thereby assigning a weight to its overall predictive power. SVM: This model classifies data by constructing a support vector hyperplane. Variable importance is evaluated by computing each feature's projection weight on the decision boundary—i.e., the coefficient weights of support vectors. A greater contribution to the hyperplane indicates a stronger predictive role in distinguishing ED from non-ED patients. KNN: As an instance-based learning method, KNN assesses variable importance by analyzing the distribution of neighboring samples. Specifically, it examines how different features influence classification based on their effect on the nearest neighbor assignments. Variables that significantly alter the classification outcome of nearby samples are deemed more influential in the model's predictions. To ensure stability and reliability in feature selection, a cross-comparison of variable importance rankings across the four models was conducted. The top ten ranked variables in all models were identified as key predictive factors. (3) Model Development and Evaluation. The selected features from the internal validation set were incorporated into predictive models based on SVM, RF, XGBoost, and KNN. These models were evaluated in terms of discrimination, calibration, and clinical utility to determine the optimal predictive approach. Discrimination: The ability of each model to distinguish between patients with and without postoperative ED was assessed using the Receiver Operating Characteristic (ROC) curve and the Area Under the Curve (AUC). AUC values range from 0.5 to 1.0, with values closer to 1.0 indicating superior discriminatory performance, meaning the model more accurately differentiates high-risk from low-risk patients. Calibration: Calibration curves were employed to compare predicted probabilities with actual outcomes. A calibration curve closely aligned with the 45° diagonal suggests that the model's predictions closely match real-world observations. Additionally, the Brier Score was computed to account for both prediction accuracy and calibration quality, with lower values indicating better overall predictive performance. Clinical Utility: Decision Curve Analysis (DCA) was used to assess the net benefit of different predictive models across varying decision thresholds. DCA determines whether a model provides additional clinical value compared to universal intervention (treating all patients) or universal non-intervention (treating none). A model with a higher net benefit across clinically relevant thresholds is considered more practical for decision-making. To enhance model robustness and mitigate bias due to data partitioning, k-fold cross-validation was performed (typically $k = 10$). The internal validation set was randomly divided into k equal-sized subsets, with k-1 subsets used for training and the remaining subset reserved for testing. This process was repeated k times, ensuring that each data point was used for testing exactly once. In each iteration, predictive models were trained using SVM, RF, XGBoost, and KNN, and evaluation metrics such as AUC were computed. The final model performance was assessed

by averaging results across k iterations, providing a robust estimate of model stability and generalizability, guiding the selection of the optimal model for further analysis. (4) External Validation. The best-performing model was applied to the external test set, composed of prostate cancer patients from The Affiliated Huaian No. 1 People's Hospital during the same period, independent of the internal validation cohort. ROC curves were generated to evaluate the model's generalization performance and predictive efficacy on an independent dataset, ensuring its applicability across different patient populations. (5) Model Interpretation. To elucidate the model's decision-making process, SHapley Additive exPlanations (SHAP) analysis was employed to quantify the contribution of each feature to the model's predictions based on Shapley values. The SHAP summary plot provided an overview of feature importance and impact direction across all samples. The horizontal axis represented the magnitude of Shapley values, with larger values indicating greater influence on prediction outcomes. The vertical axis listed features ranked by importance. Color coding (e.g., red for high values and blue for low values) visually illustrated how specific feature values influenced prediction probabilities. For individual patient predictions, single-sample SHAP force plots were generated. Positive contributions (risk-increasing factors) were depicted by red arrows, while negative contributions (risk-reducing factors) were indicated by blue arrows, offering an intuitive representation of the model's decision rationale.

3 Results

3.1 Basic clinical information of the patient

A total of 1,147 prostate cancer patients were included in this study (Fig. 1), among whom 285 (24.85%) developed postoperative ED. Univariate and multivariate analyses identified age, smoking history, Gleason score, prostate volume, T-stage, surgical procedure, surgery duration, intraoperative bleeding, and PCT level as independent risk factors for postoperative ED ($P < 0.05$) (Table 1). Feature selection using XGBoost, RF, SVM, and KNN further highlighted key risk factors, including advanced age, smoking history, Gleason score ≥ 8, prostate volume ≥ 40 mL, T-stage, laparoscopic-assisted surgery, and prolonged operative duration (Fig. 2A-D). The original dataset used in this study is provided in Table S1.

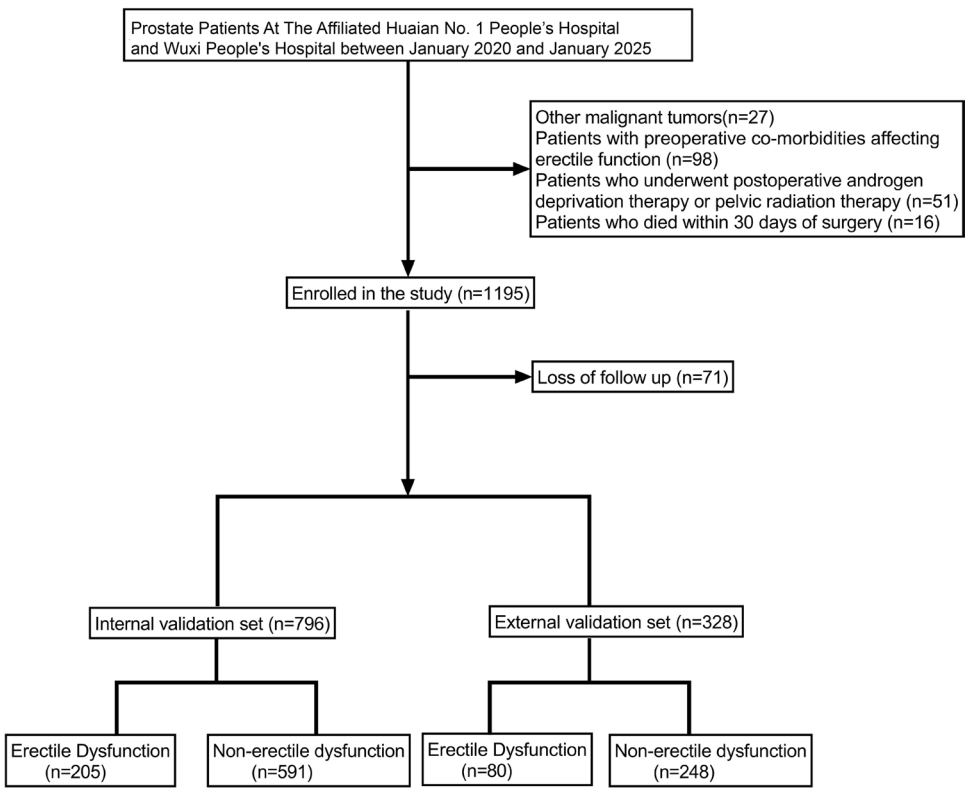

Fig. 1 Flowchart of patient inclusion in the study

Table 1 Univariate and multivariate analyses of variables related to ED

Variables		Univariate analysis		Multivariate analysis	
		OR, 95%CI	P-value	OR, 95%CI	P-value
Age	< 65	Reference		Reference	
	≥ 65	2.76 (1.99–3.83)	< 0.001	2.31 (1.21–4.44)	0.012
BMI	< 25 kg/m^2	Reference			
	≥ 25 kg/m^2	1.21 (0.86–1.71)	0.276		
ASA	< 3	Reference			
	≥ 3	0.93 (0.66–1.30)	0.664		
ALB	≥ 30 g/l	Reference			
	< 30 g/l	1.19 (0.86–1.65)	0.291		
NRS2002 score	< 3	Reference			
	≥ 3	0.74 (0.53–1.04)	0.079		
Family history	No	Reference			
	Yes	1.02 (0.67–1.55)	0.922		
Drinking history	No	Reference			
	Yes	1.22 (0.86–1.74)	0.272		
Smoking history	No	Reference		Reference	
	Yes	8.34 (5.85–11.90)	< 0.001	10.83 (5.40–21.75)	< 0.001
Anemia	No	Reference			
	Yes	1.27 (0.87–1.86)	0.213		
Hyperlipidemia	No	Reference			
	Yes	1.14 (0.77–1.68)	0.528		
Hypertension	No	Reference			
	Yes	1.31 (0.91–1.88)	0.148		
Diabetes	No	Reference		Reference	
	Yes	1.87 (1.29–2.70)	< 0.001	1.59 (0.75–3.37)	0.227
CHD	No	Reference			
	Yes	1.65 (0.97–2.82)	0.066		
Gleason Score	< 8	Reference		Reference	
	≥ 8	15.28 (10.22–22.82)	< 0.001	25.57 (11.91–54.87)	< 0.001
Cancer tissue invasion site	Non-tip or bottom	Reference			
	Tip or bottom	1.25 (0.82–1.92)	0.303		
Prostate volume	< 40 ml	Reference		Reference	
	≥ 40 ml	7.26 (5.09–10.35)	< 0.001	9.93 (4.89–20.19)	< 0.001
T-stage	T1	Reference		Reference	
	T2	9.66 (6.59–14.17)	< 0.001	12.61 (6.07–26.22)	< 0.001
Preoperative PSA	< 20 ng/ml	Reference			
	≥ 20 ng/ml	1.11 (0.71–1.73)	0.659		
Postoperative PSA	< 0.2 ng/ml	Reference			
	≥ 0.2 ng/ml	0.85 (0.52–1.38)	0.503		
Surgical procedure	Robotic surgery	Reference		Reference	
	Laparoscopic surgery	5.90 (4.19–8.32)	< 0.001	7.22 (3.64–14.32)	< 0.001
Surgery time	< 270 min	Reference		Reference	
	≥ 270 min	13.55 (9.20–19.95)	< 0.001	15.87 (7.65–32.93)	< 0.001
Intraoperative bleeding	≥ 100 ml	Reference		Reference	
	< 100 ml	0.58 (0.41–0.81)	0.001	0.51 (0.26–0.99)	0.048
PCT level	< 0.05 ng/ml	Reference		Reference	
	≥ 0.05 ng/ml	2.03 (1.41–2.93)	< 0.001	2.17 (1.05–4.52)	0.038
CRP level	< 10 mg/l	Reference		Reference	
	≥ 10 mg/l	1.67 (1.14–2.45)	0.009	1.81 (0.82–3.98)	0.14
SAA level	< 10 mg/l	Reference			
	≥ 10 mg/l	1.34 (0.93–1.94)	0.121		
NLR	< 3	Reference		Reference	
	≥3	1.51 (1.04–2.19)	0.032	1.33 (0.62–2.84)	0.459

Table 1 (continued)

OR, odds ratio; CI, confidence interval; BMI, body mass index; ASA, The American Society of Anesthesiologists; ALB, albumin; PCT, procalcitonin; CRP, C-reactive protein; NLR, neutrophil to lymphocyte ratio; SAA, serum amyloid A; NRS2002, nutrition risk screening 2002

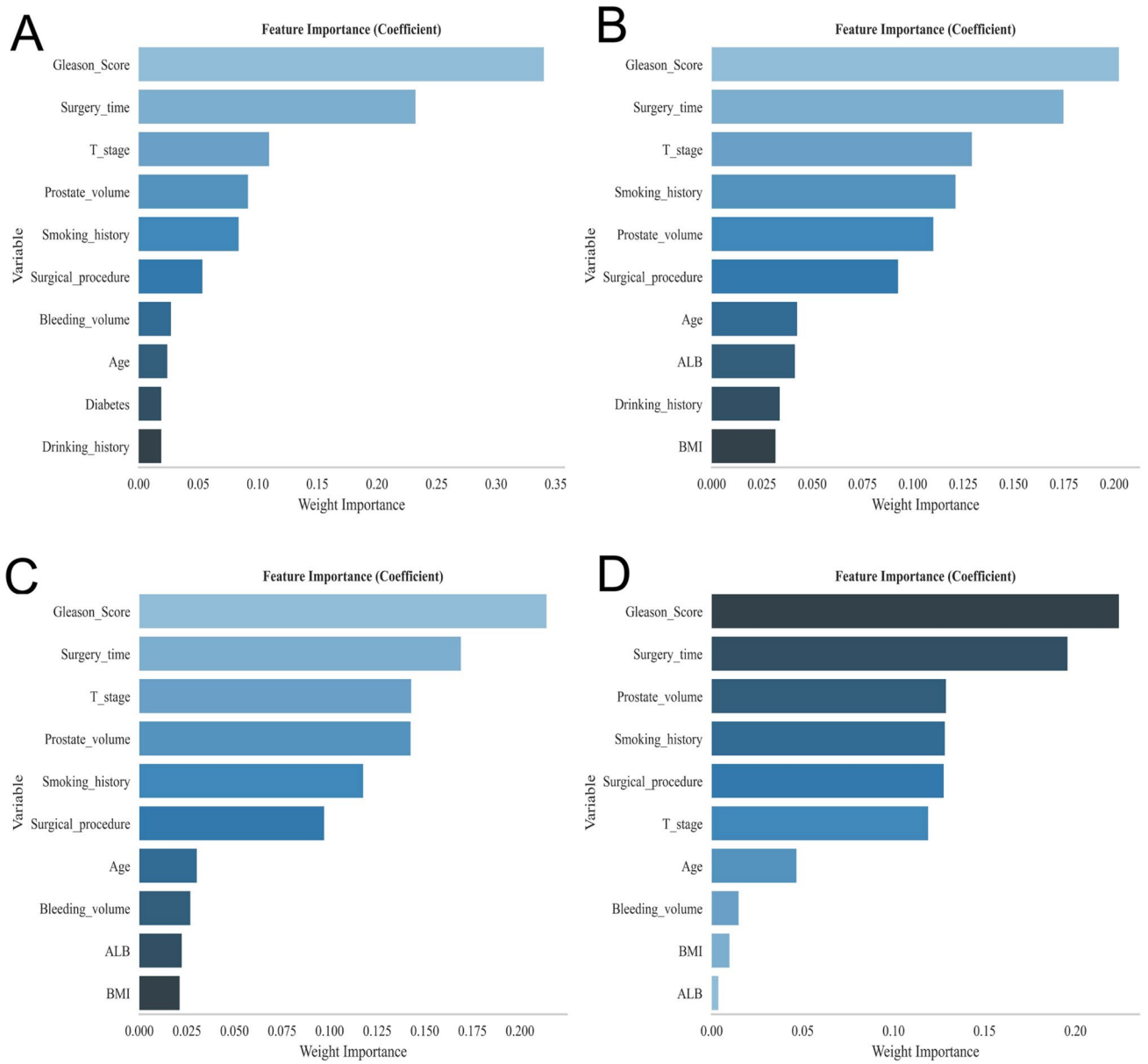

Fig. 2 Ranking of variable importance across the four models. **A** XGBoost model. **B** RF model. **C** SVM model. **D** KNN model

3.2 Model building and evaluation

ROC curve analysis demonstrated that the XGBoost model exhibited superior predictive performance in both the training and validation cohorts, achieving an AUC of 0.980 in the training set and 0.960 in the validation set, outperforming the other three machine learning models (Table 2). The high AUC values indicate that the model possesses remarkable discriminatory ability, effectively distinguishing high-risk from low-risk patients, thereby reflecting its high predictive accuracy. Furthermore, calibration curves revealed that the predictions of XGBoost, RF, SVM, and KNN closely aligned with the ideal calibration line, suggesting that these models not only excel in risk stratification but also maintain robust reliability in probability estimation. To assess clinical utility, DCA was performed. The results

Table 2 Evaluation of the performance of the four models

		AUC(95%CI)	Accuracy(95%CI)	Sensitivity(95%CI)	Specificity(95%CI)	F1 score(95%CI)
KNN	Training set	0.97 (0.96–0.99)	0.94(0.93–0.94)	0.9(0.88–0.91)	0.95(0.95–0.96)	0.88(0.87–0.89)
	Validation set	0.93 (0.88–0.98)	0.9(0.89–0.91)	0.8(0.77–0.83)	0.94(0.92–0.95)	0.8(0.79–0.82)
XGBoost	Training set	0.98 (0.98–0.99)	0.94(0.94–0.95)	0.92(0.91–0.93)	0.95(0.94–0.96)	0.89(0.89–0.90)
	Validation set	0.96 (0.93–0.99)	0.91(0.89–0.92)	0.86(0.82–0.91)	0.93(0.91–0.94)	0.83(0.80–0.85)
RF	Training set	0.97 (0.96–0.99)	0.93(0.92–0.93)	0.93(0.92–0.95)	0.92(0.91–0.93)	0.87(0.86–0.88)
	Validation set	0.89 (0.82–0.96)	0.89(0.88–0.90)	0.85(0.81–0.88)	0.91(0.89–0.93)	0.8(0.78–0.82)
SVM	Training set	0.98 (0.96–0.99)	0.94(0.93–0.95)	0.91(0.89–0.92)	0.95(0.94–0.96)	0.89(0.87–0.90)
	Validation set	0.96 (0.93–0.99)	0.91(0.90–0.93)	0.86(0.83–0.90)	0.93(0.92–0.94)	0.84(0.81–0.86)

CI, confidence interval

demonstrated that, compared to the "treat-all" or "treat-none" strategies, all machine learning models provided higher net clinical benefit (Fig. 3A-D). Notably, XGBoost exhibited the most favorable performance, underscoring its potential to deliver precise and individualized risk prediction for postoperative erectile dysfunction in patients undergoing radical prostatectomy. To comprehensively evaluate the generalization performance of the four machine learning models, we employed k-fold cross-validation within the internal validation cohort. Specifically, 540 samples (67.84%) were randomly selected as the test set, while the remaining samples were used for training, and a tenfold cross-validation was conducted. This approach enabled a more robust assessment of each model's performance across different data subsets, mitigating potential biases from data partitioning and enhancing model stability and reliability. During cross-validation, the XGBoost model outperformed the other models, achieving a mean AUC of 0.9127 ± 0.0770 in the validation set, an AUC of 0.9592 in the test set, and an accuracy of 0.9111. These findings suggest that XGBoost maintains consistent predictive performance across different datasets, demonstrating superior generalization capability. Comparatively, the other three models exhibited slightly inferior performance: RF achieved a validation AUC of 0.8990 ± 0.0692, a test AUC of 0.9141, and an accuracy of 0.7704, indicating strong discriminative ability but lower accuracy, potentially leading to misclassification in certain cases. Support Vector Machine (SVM) attained a validation AUC of 0.9080 ± 0.0523, a test AUC of 0.9186, and an accuracy of 0.9019, demonstrating strong predictive performance, albeit slightly below XGBoost. KNN yielded a validation AUC of 0.8922 ± 0.0678, a test AUC of 0.9236, and an accuracy of 0.8148. Although KNN achieved the highest AUC in the test set, its overall accuracy remained lower than XGBoost, suggesting potential limitations in high-dimensional data settings. Collectively, XGBoost outperformed all models across evaluation metrics, particularly excelling in AUC and accuracy, indicating superior discriminative power, generalization ability, and stable predictive performance. Therefore, XGBoost was ultimately selected as the optimal algorithm for predicting high-risk factors for postoperative erectile dysfunction. For external validation, we further assessed the model's generalization ability using ROC curve analysis, which yielded an AUC of 0.84 (Fig. 4A-D). This result confirms that the model maintains high predictive accuracy on previously unseen data, demonstrating strong external validity and clinical applicability.

3.3 Model explanation

The SHAP summary plot (Fig. 5) illustrates the key risk factors for postoperative ED and their relative contributions. The results indicate that larger prostate volume, Gleason Score ≥ 8, T2-stage tumors, prolonged operative time, history of smoking, laparoscopic-assisted surgery, and advanced age are the most significant predictors of ED. To further validate the clinical applicability of the model, we analyzed four individual patients using SHAP force plots (Fig. 6A-D) to reveal their specific high-risk factors and contribution levels:

Patient 1: The model predicted an ED probability of 0.83, primarily driven by advanced age, larger prostate volume, laparoscopic-assisted surgery, and smoking history. The accumulation of these high-risk factors resulted in a substantially increased ED risk. Patient 2: The model estimated an ED probability of just 0.01, suggesting an extremely low risk. Patient 3: The predicted ED probability was 0.40, with Gleason Score ≥ 8 and larger prostate volume identified as the key

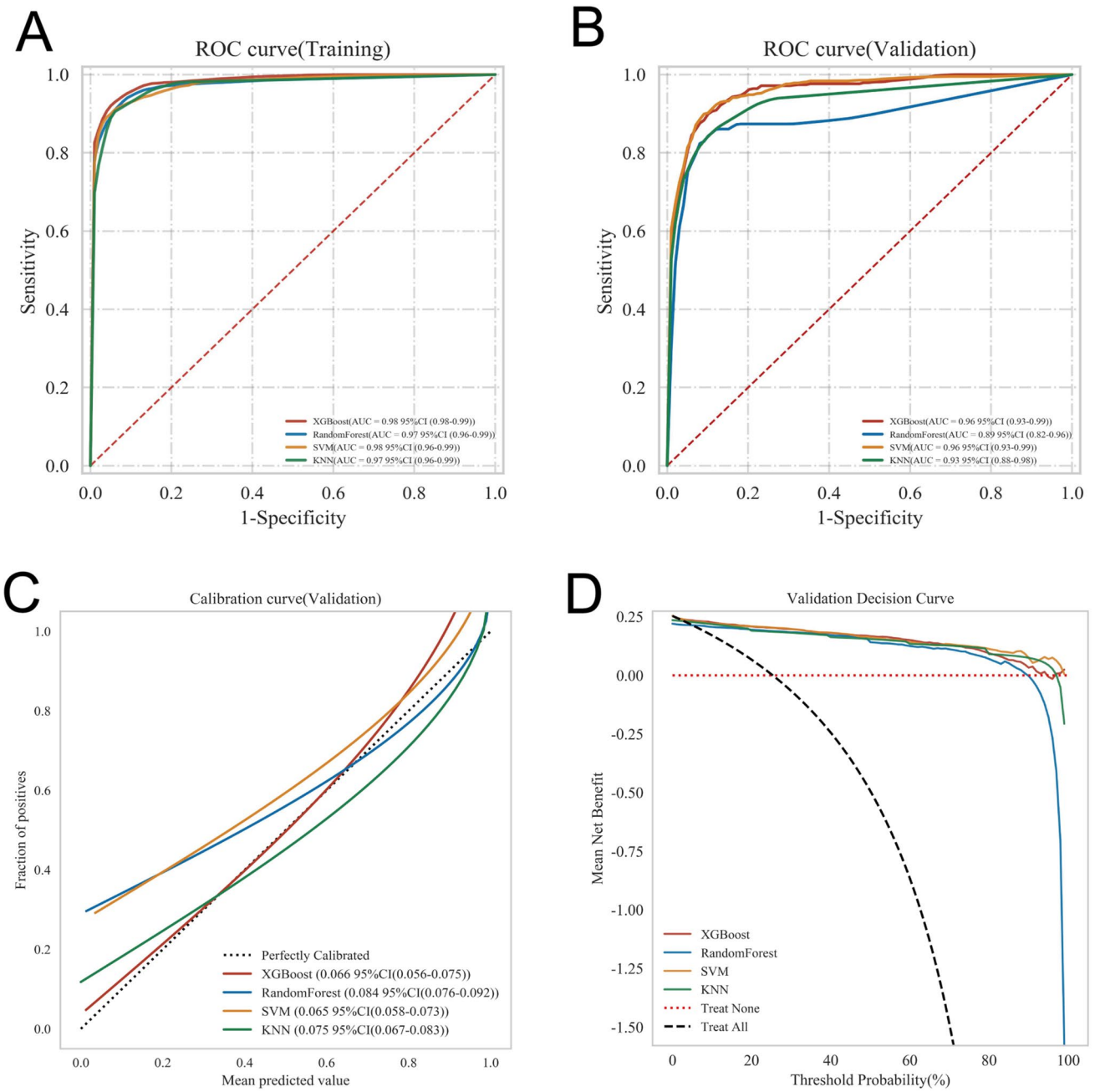

Fig. 3 Predictive performance assessment of the four models. **A** ROC curves for the training set. **B** ROC curves for the validation set. **C** Calibration plots, where the 45° dotted line represents perfect agreement between predicted and observed probabilities, with closer alignment indicating higher accuracy. **D** Decision curve analysis (DCA), where the intersection of the red curve with the "All" curve marks the starting point, and its intersection with the "None" curve defines the range within which patients benefit

contributing factors. While these factors elevate the risk, the overall probability remains moderate. Patient 4: The model estimated an ED probability of 0.21, mainly influenced by age ≥ 65 years, smoking history, and prolonged operative time. Although the risk is relatively low, close monitoring remains warranted.

These individualized SHAP analyses highlight the model's interpretability, enabling personalized risk stratification and facilitating targeted clinical decision-making.

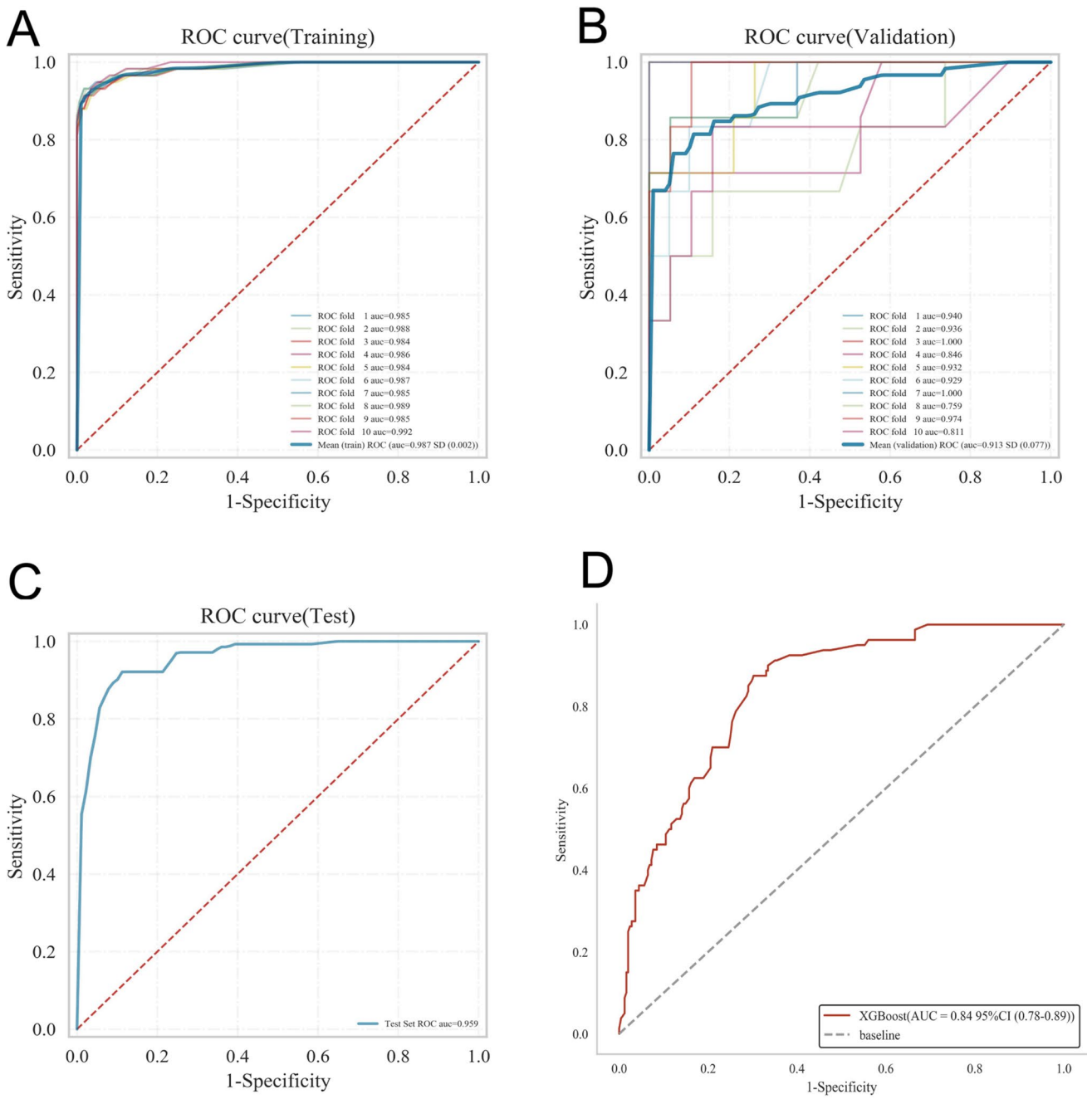

Fig. 4 Internal and external validation of the XGBoost model. **A** ROC curve for the training set. **B** ROC curve for the validation set. **C** ROC curve for the test set. **D** External validation results

4 Discussion

Traditional statistical methods and empirical assessments have long dominated risk prediction in complex and challenging clinical scenarios. However, their limitations are becoming increasingly evident [24, 25]. Empirical approaches heavily rely on clinicians' individual experience, making them susceptible to cognitive biases such as representativeness bias and recall bias. Clinicians may overemphasize certain intuitive factors while overlooking critical latent variables, such as subtle variations in operative time or refinements in nerve-sparing techniques. Furthermore, experience-driven predictions struggle to dynamically integrate new evidence or surgical innovations, causing predictive models to lag behind advancements in clinical practice.

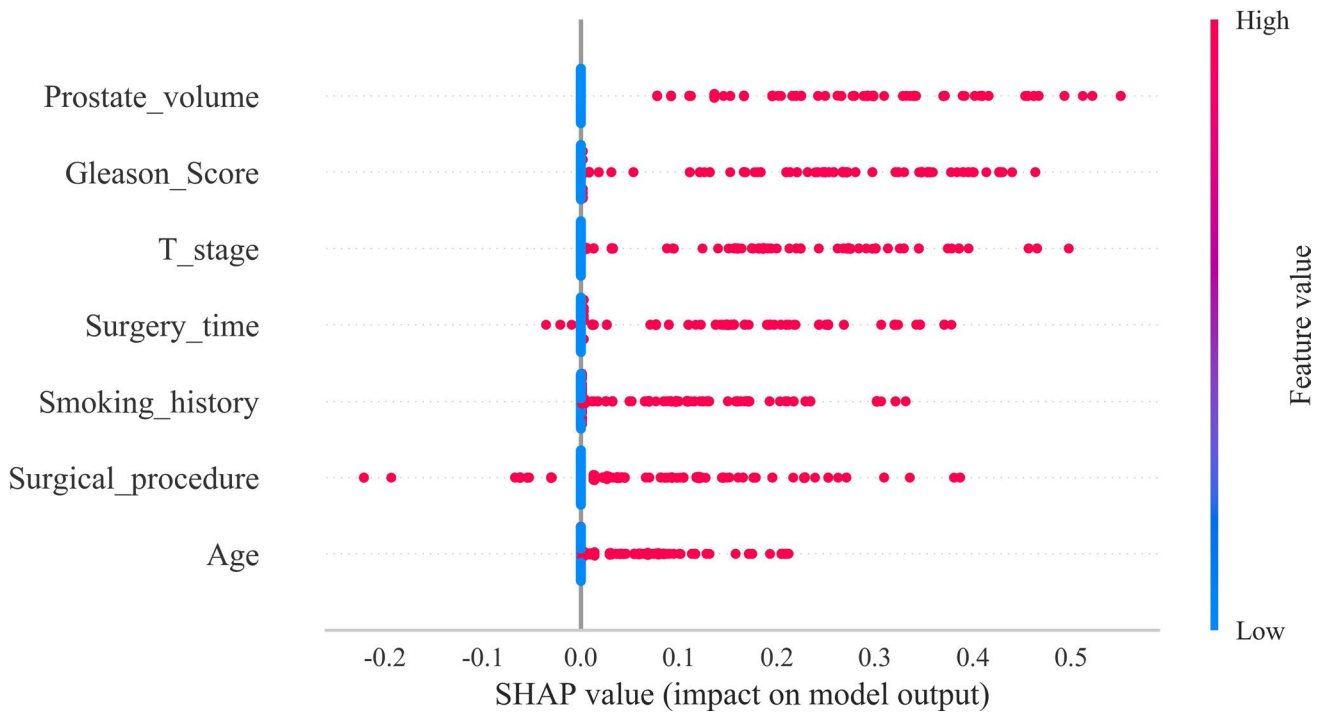

Fig. 5 SHAP summary plot illustrating the contribution of risk factors, ranked by the mean absolute Shapley values. Higher-positioned factors have a greater impact on model predictions

Similarly, traditional statistical methods, such as logistic regression, operate under linear assumptions, making them inadequate for capturing complex nonlinear interactions between variables like age and BMI, which are often crucial in disease pathogenesis [26, 27]. Additionally, these methods rely on researcher-driven variable selection, which may omit key predictive factors or introduce multicollinearity, thereby compromising model robustness. The rise of high-dimensional clinical data, including multiparametric MRI features and molecular biomarkers, further highlights the inherent limitations of traditional models in handling advanced feature extraction and selection.

In this study, we harnessed four machine learning algorithms—XGBoost, RF, SVM, and KNN—to rigorously assess their predictive efficacy in delineating high-risk factors for postoperative ED following radical prostatectomy. Each algorithm confers distinct methodological advantages: XGBoost, a gradient boosting-based ensemble approach, excels in navigating high-dimensional data landscapes and unraveling intricate feature interdependencies, such as prostate volume and Gleason score, while simultaneously mitigating overfitting. Its tree-structured optimization strategy, including greedy feature partitioning, augments sensitivity to pivotal risk determinants, such as advanced age and prolonged operative duration. Notably, XGBoost exhibited the most robust predictive performance, attaining a test-set AUC of 0.9592 and a cross-validation accuracy of 0.9111, alongside an external validation AUC of 0.84, underscoring its formidable generalization capability across heterogeneous datasets [28, 29]. RF, which aggregates multiple decision trees through an ensemble voting paradigm, effectively curtails overfitting [30]. However, despite its robust feature importance ranking via out-of-bag error estimation, RF's stochastic subspace sampling may inadvertently exclude critical feature synergies. SVM, which delineates decision boundaries via hyperplanes in high-dimensional feature space, demonstrated commendable predictive proficiency (test-set AUC = 0.9186); nevertheless, its reliance on meticulous hyperparameter calibration and computational intensity in large-scale datasets constrain its clinical applicability. KNN, an instance-based classifier, exhibited robust performance in lower-dimensional scenarios (test-set AUC = 0.9236); however, its dependence on local similarity metrics hampers adaptability to noisy data and exacerbates susceptibility to high-dimensional sparsity, yielding an accuracy of 0.8148—substantially inferior to XGBoost [31, 32]. Our findings unequivocally establish XGBoost as the superior predictive model, consistently surpassing its counterparts across training, validation, and external validation datasets. Its capacity to accurately stratify high-risk and low-risk patients, while maintaining stable predictive efficacy across diverse cohorts, further reinforces its clinical applicability. Moreover, calibration curve analysis substantiated the strong concordance between XGBoost's probabilistic predictions and actual outcomes, while DCA affirmed its tangible clinical utility in informing decision-making processes. Collectively, these attributes position XGBoost as the preeminent

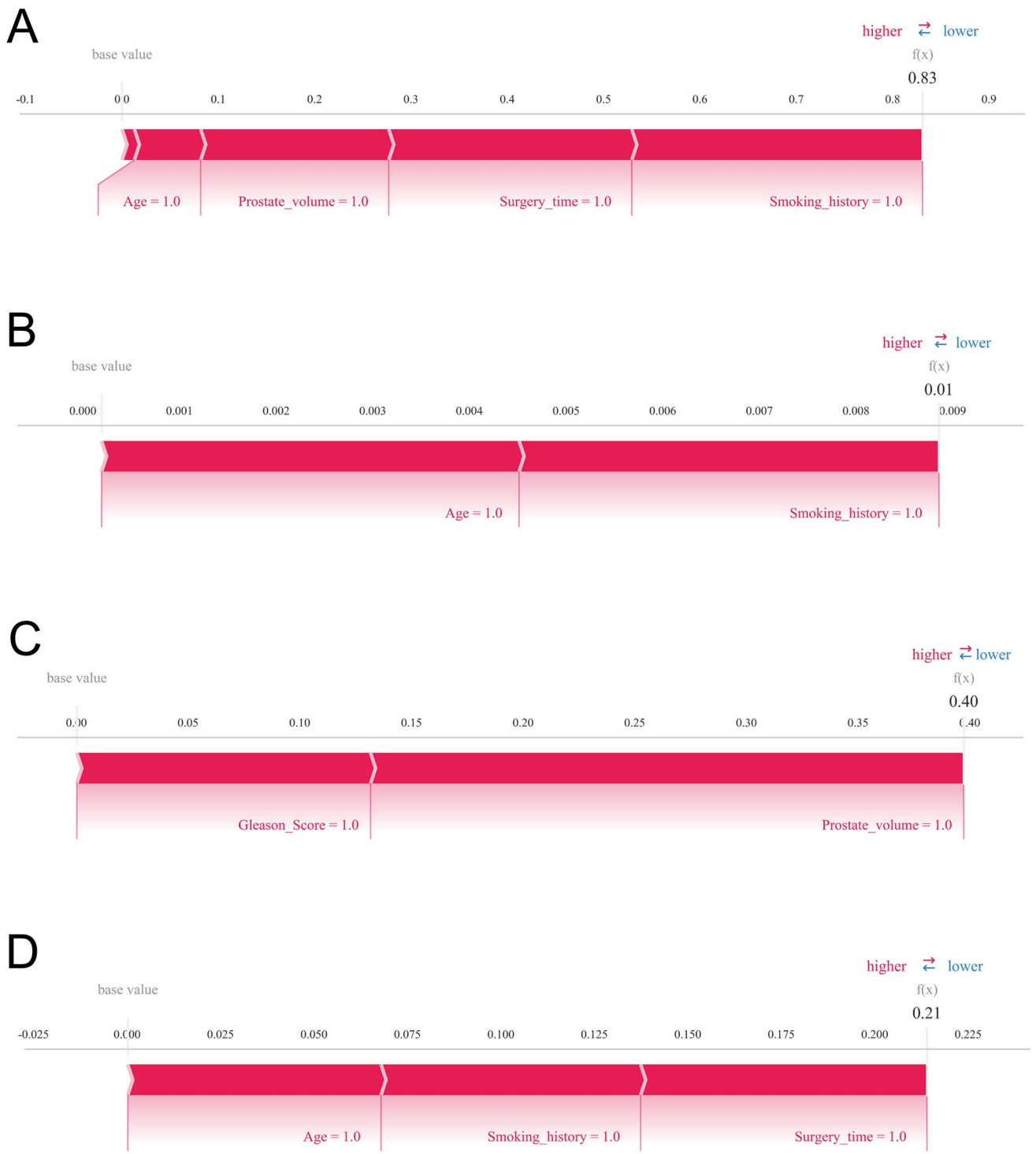

Fig. 6 SHAP force plot visualizing individual predictions. Variables are arranged horizontally based on their absolute influence. Blue indicates a negative effect on disease prediction (decreasing SHAP values), while red indicates a positive effect (increasing SHAP values). **A** Patient I. **B** Patient II. **C** Patient III. **D** Patient IV

model for forecasting high-risk factors for postoperative ED, offering a powerful conduit for precision medicine and individualized therapeutic strategies.

Our ED risk prediction model offers broad applicability across diverse clinical scenarios, encompassing preoperative planning, intraoperative guidance, and postoperative management. During the initial physical examination or outpatient screening, the model enables the early identification of high-risk individuals, prompting timely recommendations for

advanced imaging. In the preoperative phase, it assists in stratifying patient risk in anticipation of prostate cancer-related therapies, thereby informing the development of tailored treatment strategies, including the preoperative adjustment of metabolic therapy regimens for high-risk individuals. Furthermore, for patients predisposed to ED following prostate cancer surgery, the model supports the optimization of preoperative management and provides critical insights during treatment, guiding clinicians in refining therapeutic approaches—such as modifying radiotherapy or chemotherapy protocols—to mitigate ED risk. In the postoperative setting, the model facilitates the implementation of personalized surveillance strategies, incorporating routine imaging and biochemical monitoring, and proves particularly valuable for the long-term follow-up of prostate cancer survivors to continuously evaluate the risk of ED and associated complications.

In this study, we employed SHAP analysis to elucidate the model's predictive mechanisms, highlighting prostate volume as a critical determinant of postoperative ED. The autonomic innervation governing erectile function, composed of sympathetic and parasympathetic fibers, is primarily situated laterally and posteriorly to the prostate, traversing the neurovascular bundles (NVBs) [33, 34]. Although all patients in this study underwent nerve-sparing radical prostatectomy, glandular hypertrophy may induce anatomical displacement of the NVBs, bringing them into closer proximity to the surgical resection margin. This spatial shift increases the susceptibility of these delicate neural structures to inadvertent intraoperative trauma, thereby compromising erectile function. Furthermore, prostate enlargement may distort adjacent anatomical relationships, potentially embedding the NVBs within the prostatic capsule and rendering nerve preservation technically more arduous, further amplifying the risk of iatrogenic injury. Additionally, in cases of substantial prostate hypertrophy, the surgical field may be obstructed, necessitating prolonged operative durations for bladder neck dissection, prostate excision, and urethral reconstruction. Extended surgical times, in turn, contribute to heightened local inflammation and tissue edema, which may delay postoperative neurovascular recovery and exacerbate the likelihood of ED.

Additionally, we observed that robot-assisted surgery confers substantial advantages over conventional laparoscopic approaches, offering superior intraoperative precision, enhanced nerve preservation, reduced blood loss, and improved pelvic floor integrity—factors that collectively contribute to a significantly lower incidence of postoperative ED. The robotic system provides a 10 × high-definition three-dimensional (3D) visualization, affording surgeons unparalleled clarity in identifying and preserving the NVBs [12, 35]. Given the NVBs' pronounced vulnerability to ischemia and hypoxia, excessive intraoperative hemorrhage may impair penile corpus cavernosum perfusion, exacerbating the risk of postoperative ED. Compared to the two-dimensional (2D) perspective of laparoscopic surgery, robotic-assisted systems facilitate superior differentiation of the prostate from adjacent structures, thereby mitigating the risk of inadvertent injury to the parasympathetic and sympathetic nerves integral to erectile function while simultaneously minimizing intraoperative blood loss [36]. Moreover, the robotic system's multi-degree-of-freedom articulated instruments, capable of 540° rotation, surpass the dexterity of conventional laparoscopic tools, enabling meticulous NVB dissection with minimal traction and nerve disruption, thereby optimizing erectile function preservation. Crucially, robotic-assisted surgery also allows for precise bladder neck division and urethral anastomosis, reducing iatrogenic trauma to periprostatic neural structures and lowering the likelihood of postoperative urinary incontinence. The resultant improvement in continence recovery alleviates patient anxiety, indirectly bolstering erectile function. Furthermore, emerging evidence underscores the pivotal role of the pelvic floor musculature in maintaining penile erection. By minimizing excessive traction and inadvertent injury to pelvic structures, the refined surgical precision afforded by robotic systems fosters superior postoperative erectile function recovery.

In this study, we further employed four representative cases to elucidate how the model predicts the risk of postoperative ED. Notably, in Case 3, Gleason grading emerged as a pivotal determinant. As a histopathological indicator of prostate cancer aggressiveness, a higher Gleason score is often indicative of more invasive tumor biology [37]. We hypothesize that elevated Gleason scores are frequently associated with NVB invasion, necessitating more extensive surgical excision to mitigate the risk of residual disease and recurrence [38]. Furthermore, high-grade prostate cancer is more likely to provoke localized inflammation and postoperative fibrosis, both of which hinder nerve regeneration, thereby compromising erectile function recovery [39, 40]. Beyond Gleason grading, tumor staging (T-stage) also plays a crucial role in delineating the extent of local tumor spread, significantly influencing postoperative ED risk. In T2-stage localized prostate cancer, although the malignancy remains confined within the prostate, its extension into one or both lobes heightens the likelihood of NVB involvement. Even in nerve-sparing procedures, intraoperative manipulation may induce mechanical trauma, ischemia, or traction-related injury to the NVBs, thereby further impeding postoperative erectile function restoration.

Despite leveraging machine learning to elucidate the factors influencing ED following radical prostatectomy and providing valuable clinical insights, this study has several limitations that warrant further refinement and investigation.

First, the retrospective design inherently carries a risk of selection bias, as it relies on historical medical records that may be incomplete for certain variables. Additionally, variability in patient adherence to follow-up protocols could impact the reliability of the conclusions. The relatively modest sample size may further compromise the external validity of the findings, potentially introducing bias in the analysis. Notably, preoperative erectile function was assessed using the IIEF-5 score, a self-reported measure prone to subjective bias. Psychological factors, cultural background, and social influences may lead some patients to either overestimate or underestimate their erectile function, thereby affecting data accuracy. Moreover, the study did not incorporate objective physiological assessments, such as nocturnal penile tumescence (NPT) testing or vascular endothelial function analysis, which may have introduced further measurement inaccuracies in preoperative erectile function evaluation. Future research will focus on expanding the cohort, refining study methodologies, and integrating multicenter data, prospective follow-up, and a broader spectrum of clinical parameters. Through these enhancements, we aim to achieve a more precise assessment of the impact of nerve-sparing surgery on postoperative erectile function, ultimately providing more robust evidence to inform clinical decision-making.

5 Conclusion

Our study leveraged machine learning to construct a predictive model for ED following radical prostatectomy, demonstrating high accuracy and strong clinical applicability. Our findings highlight prostate volume as a pivotal factor in postoperative ED, likely due to its influence on the anatomical positioning of the NVB, thereby heightening the risk of intraoperative nerve injury. Moreover, robot-assisted surgery confers significant advantages over laparoscopic approaches, offering superior precision, enhanced nerve preservation, reduced intraoperative bleeding, and improved pelvic floor protection, collectively contributing to a markedly lower incidence of postoperative ED. Additionally, tumor characteristics, including Gleason score and T stage, emerged as critical risk factors. A higher Gleason score is indicative of more aggressive tumor biology, while locally advanced tumors (high T stage) exhibit a greater propensity for NVB invasion. Consequently, these patients often require a more extensive resection, elevating the likelihood of intraoperative nerve damage and prolonging postoperative functional recovery.

Author contributions Hesong Jiang, Lu Ji, Leilei Zhu, Fei Mao made a significant contribution to the conception, study design, execution, acquisition of data, analysis and interpretation, or in all these areas; Fei Mao, Hesong Jiang, and Hengbing Wang took part in drafting, revising or critically reviewing the article and gave final approval of the version to be published; All author have agreed on the journal to which the article has been submitted and agree to be accountable for all aspects of the work.

Funding The author(s) declare financial support was received for the research, authorship, and/or publication of this article. This work was supported by the Development Fund of Affiliated Hospital of Xuzhou Medical University (No. XYFY202312) and Huai'an Science and Technology Plan Project (No. HAB2024013).

Data availability The data that support the findings of this study are available from the corresponding author, upon reasonable request.

Declarations

Ethics approval and consent to participate All patients have signed an informed consent form. All procedures performed were in accordance with the declaration of the ethical standards of the institutional research committee and with the 1964 Helsinki 387 Declaration and its later amendments. The Ethics Committee of The Affiliated Huaian No. 1 People's Hospital of Nanjing Medical University has approved this study (No: KY-2024-198-01).

Consent for publication Not applicable.

Competing interests The authors declare no competing interests.

References

1. Sekhoacha M, Riet K, Motloung P, Gumenku L, Adegoke A, Mashele S. Prostate cancer review: genetics, diagnosis, treatment options, and alternative approaches. Molecules. 2022. https://doi.org/10.3390/molecules27175730.
2. Heidenreich A, Pfister D. Radical cytoreductive prostatectomy in men with prostate cancer and oligometastatic disease. Curr Opin Urol. 2020;30(1):90–7. https://doi.org/10.1097/mou.0000000000000691.
3. Sung H, Ferlay J, Siegel RL, Laversanne M, Soerjomataram I, Jemal A, et al. Global cancer statistics 2020: globocan estimates of incidence and mortality worldwide for 36 cancers in 185 countries. CA Cancer J Clin. 2021;71(3):209–49. https://doi.org/10.3322/caac.21660.
4. Bray F, Laversanne M, Sung H, Ferlay J, Siegel RL, Soerjomataram I, et al. Global cancer statistics 2022: globocan estimates of incidence and mortality worldwide for 36 cancers in 185 countries. CA Cancer J Clin. 2024;74(3):229–63. https://doi.org/10.3322/caac.21834.
5. Gandaglia G, Briganti A, Clarke N, Karnes RJ, Graefen M, Ost P, et al. Adjuvant and salvage radiotherapy after radical prostatectomy in prostate cancer patients. Eur Urol. 2017;72(5):689–709. https://doi.org/10.1016/j.eururo.2017.01.039.
6. Stewart SB, Boorjian SA. Radical prostatectomy in high-risk and locally advanced prostate cancer: mayo clinic perspective. Urol Oncol. 2015;33(5):235–44. https://doi.org/10.1016/j.urolonc.2014.10.003.
7. Shen C, Jain K, Shah T, Schaefer E, Zhou S, Fried D, et al. Relationships between erectile dysfunction, prostate cancer treatment type and inflatable penile prosthesis implantation. Investig Clin Urol. 2022;63(3):316–24. https://doi.org/10.4111/icu.20210445.
8. Mirza M, Griebling TL, Kazer MW. Erectile dysfunction and urinary incontinence after prostate cancer treatment. Semin Oncol Nurs. 2011;27(4):278–89. https://doi.org/10.1016/j.soncn.2011.07.006.
9. Liu Q, Zhang Y, Wang J, Li S, Cheng Y, Guo J, et al. Erectile dysfunction and depression: a systematic review and meta-analysis. J Sex Med. 2018;15(8):1073–82. https://doi.org/10.1016/j.jsxm.2018.05.016.
10. Yuan P, Chen Y, Sun T, Cui L, Wei Y, Li T, et al. Exploring potential genes and mechanisms linking erectile dysfunction and depression. Front Endocrinol. 2023;14:1221043. https://doi.org/10.3389/fendo.2023.1221043.
11. Bratu O, Oprea I, Marcu D, Spinu D, Niculae A, Geavlete B, et al. Erectile dysfunction post-radical prostatectomy—a challenge for both patient and physician. J Med Life. 2017;10(1):13–8.
12. Wang J, Hu K, Wang Y, Wu Y, Bao E, Wang J, et al. Robot-assisted versus open radical prostatectomy: a systematic review and meta-analysis of prospective studies. J Robot Surg. 2023;17(6):2617–31. https://doi.org/10.1007/s11701-023-01714-8.
13. Emanu JC, Avildsen IK, Nelson CJ. Erectile dysfunction after radical prostatectomy: prevalence, medical treatments, and psychosocial interventions. Curr Opin Support Palliat Care. 2016;10(1):102–7. https://doi.org/10.1097/spc.0000000000000195.
14. Irwin GM. Erectile dysfunction. Prim Care. 2019;46(2):249–55. https://doi.org/10.1016/j.pop.2019.02.006.
15. Wang W, Jing Z, Liu W, Zhu L, Ren H, Hou X. Hyperuricaemia is an important risk factor of the erectile dysfunction: a systematic review and meta-analysis. Andrologia. 2022;54(5):e14384. https://doi.org/10.1111/and.14384.
16. Zhao B, Hong Z, Wei Y, Yu D, Xu J, Zhang W. Erectile dysfunction predicts cardiovascular events as an independent risk factor: a systematic review and meta-analysis. J Sex Med. 2019;16(7):1005–17. https://doi.org/10.1016/j.jsxm.2019.04.004.
17. Li MP, Liu WC, Wu JB, Luo K, Liu Y, Zhang Y, et al. Machine learning for the prediction of postoperative nosocomial pulmonary infection in patients with spinal cord injury. Eur Spine J. 2023;32(11):3825–35. https://doi.org/10.1007/s00586-023-07772-8.
18. Wang K, Hong T, Liu W, Xu C, Yin C, Liu H, et al. Development and validation of a machine learning-based prognostic risk stratification model for acute ischemic stroke. Sci Rep. 2023;13(1):13782. https://doi.org/10.1038/s41598-023-40411-2.
19. Wang Z, Xu C, Liu W, Zhang M, Zou J, Shao M, et al. A clinical prediction model for predicting the risk of liver metastasis from renal cell carcinoma based on machine learning. Front Endocrinol. 2022;13:1083569. https://doi.org/10.3389/fendo.2022.1083569.
20. Ying H, Guo BW, Wu HJ, Zhu RP, Liu WC, Zhong HF. Using multiple indicators to predict the risk of surgical site infection after orif of tibia fractures: a machine learning based study. Front Cell Infect Microbiol. 2023;13:1206393. https://doi.org/10.3389/fcimb.2023.1206393.
21. Rosen RC, Riley A, Wagner G, Osterloh IH, Kirkpatrick J, Mishra A. The international index of erectile function (Iief): a multidimensional scale for assessment of erectile dysfunction. Urology. 1997;49(6):822–30. https://doi.org/10.1016/s0090-4295(97)00238-0.
22. Rosen RC, Cappelleri JC, Smith MD, Lipsky J, Peña BM. Development and evaluation of an abridged, 5-item version of the international index of erectile function (iief-5) as a diagnostic tool for erectile dysfunction. Int J Impot Res. 1999;11(6):319–26. https://doi.org/10.1038/sj.ijir.3900472.
23. Mi Z, Liu J, Wang L, Luo Y, Yang K. Screening of associated factors for erectile dysfunction after radical prostatectomy and construction of a clinical risk assessment model: a retrospective study. Arch Esp Urol. 2024;77(1):92–7. https://doi.org/10.56434/j.arch.esp.urol.20247701.12.
24. Nguyen HMT, Gabrielson AT, Hellstrom WJG. Erectile dysfunction in young men-a review of the prevalence and risk factors. Sex Med Rev. 2017;5(4):508–20. https://doi.org/10.1016/j.sxmr.2017.05.004.
25. Zhang J, Shi W, Zou M, Zeng Q, Feng Y, Luo Z, et al. Prevalence and risk factors of erectile dysfunction in Covid-19 patients: a systematic review and meta-analysis. J Endocrinol Invest. 2023;46(4):795–804. https://doi.org/10.1007/s40618-022-01945-w.
26. Wang W, Xiang LY, Ma YC, Chen JW, Peng L, Gao XS, et al. The association between heavy metal exposure and erectile dysfunction in the United States. Asian J Androl. 2023;25(2):271–6. https://doi.org/10.4103/aja202237.
27. Wang W, Ma Y, Chen J, Peng L, Gao X, Lin L, et al. The association between 2, 4-dichlorophenoxyacetic acid and erectile dysfunction. Front Public Health. 2022;10:910251. https://doi.org/10.3389/fpubh.2022.910251.
28. Li J, Liu S, Hu Y, Zhu L, Mao Y, Liu J. Predicting mortality in intensive care unit patients with heart failure using an interpretable machine learning model: retrospective cohort study. J Med Internet Res. 2022;24(8):e38082. https://doi.org/10.2196/38082.
29. Li F, Xin H, Zhang J, Fu M, Zhou J, Lian Z. prediction model of in-hospital mortality in intensive care unit patients with heart failure: machine learning-based, retrospective analysis of the mimic-Iii database. BMJ Open. 2021;11(7):e044779. https://doi.org/10.1136/bmjopen-2020-044779.
30. Li C, Liu M, Zhang Y, Wang Y, Li J, Sun S, et al. Novel models by machine learning to predict prognosis of breast cancer brain metastases. J Transl Med. 2023;21(1):404. https://doi.org/10.1186/s12967-023-04277-2.

31. Li J, Luo Y, Dong M, Liang Y, Zhao X, Zhang Y, et al. Tree-based risk factor identification and stroke level prediction in stroke cohort study. Biomed Res Int. 2023;2023:7352191. https://doi.org/10.1155/2023/7352191.
32. Peng Y, Yu GI. Model Multifactor Analysis of Soil Heavy Metal Pollution on Plant Germination in Southeast Chengdu, China: Based on Redundancy Analysis, Factor Detector, and Xgboost-Shap. Sci Total Environ. 2024;954:176605. https://doi.org/10.1016/j.scitotenv.2024.176605.
33. Qalawena MM, Al-Shatouri MA, Motawaa MA, El-Sakka AI. Association between prostate zonal volume and erectile dysfunction in patients with benign prostatic hyperplasia. Sex Med. 2020;8(2):205–13. https://doi.org/10.1016/j.esxm.2020.01.008.
34. Hanna K, Arthur M, Welliver C. Erectile dysfunction and prostate diseases are the predominant google search terms amongst men's health topics. Int J Impot Res. 2022;34(6):552–7. https://doi.org/10.1038/s41443-021-00448-1.
35. Arenas-Gallo C, Shoag JE, Hu JC. Optimizing surgical techniques in robot-assisted radical prostatectomy. Urol Clin North Am. 2021;48(1):1–9. https://doi.org/10.1016/j.ucl.2020.09.002.
36. Haney CM, Kowalewski KF, Westhoff N, Holze S, Checcuci E, Neuberger M, et al. Robot-assisted versus conventional laparoscopic radical prostatectomy: a systematic review and meta-analysis of randomised controlled trials. Eur Urol Focus. 2023;9(6):930–7. https://doi.org/10.1016/j.euf.2023.05.007.
37. de Lira GHS, Fornari A, Cardoso LF, Aranchipe M, Kretiska C, Rhoden EL. Effects of perioperative pelvic floor muscle training on early recovery of urinary continence and erectile function in men undergoing radical prostatectomy: a randomized clinical trial. Int Braz J Urol. 2019;45(6):1196–203. https://doi.org/10.1590/s1677-5538.Ibju.2019.0238.
38. Lin CY, Burri A, Pakpour AH. Premature ejaculation and erectile dysfunction in iranian prostate cancer patients. Asian Pac J Cancer Prev. 2016;17(4):1961–6. https://doi.org/10.7314/apjcp.2016.17.4.1961.
39. Alchin DR, Murphy D, Lawrentschuk N. Risk factors for gleason score upgrading following radical prostatectomy. Minerva Urol Nefrol. 2017;69(5):459–65. https://doi.org/10.23736/s0393-2249.16.02684-9.
40. Swanson GP, Trevathan S, Hammonds KAP, Speights VO, Hermans MR. Gleason score evolution and the effect on prostate cancer outcomes. Am J Clin Pathol. 2021;155(5):711–7. https://doi.org/10.1093/ajcp/aqaa130.